STEM CELLS TRANSLATIONAL MEDICINE®

TISSUE ENGINEERING AND REGENERATIVE MEDICINE

NG2+ Progenitors Derived From Embryonic Stem Cells Penetrate Glial Scar and Promote Axonal Outgrowth Into White Matter After Spinal Cord Injury

SUDHAKAR VADIVELU,[a] TODD J. STEWART,[b] YUN QU,[a] KEVIN HORN,[c] SU LIU,[a] QUN LI,[a] JERRY SILVER,[c] JOHN W. MCDONALD[a,d]

Key Words. Differentiation • Glia • Matrix metalloproteinase • Plasticity • Neural progenitor • Central nervous system • Spinal cord injury • Glial scar • Axonal regeneration

[a]The International Center for Spinal Cord Injury, Hugo W. Moser Research Institute at the Kennedy Krieger Institute, Baltimore, Maryland, USA; [b]Department of Neurosurgery, Washington University School of Medicine, St. Louis, Missouri, USA; [c]Department of Neurosciences, Case Western Reserve University School of Medicine, Cleveland, Ohio, USA; [d]Department of Neurology and Neuroscience, Johns Hopkins University School of Medicine, Baltimore, Maryland, USA

Correspondence: Sudhakar Vadivelu, D.O., Division of Neurosurgery, Cincinnati Children's Hospital Medical Center and the Department of Neurosurgery, University of Cincinnati College of Medicine, 3333 Burnet Avenue, MLC 2016, Cincinnati, Ohio 45229, USA. Telephone: 513-636-4726; E-Mail: Sudhakar.Vadivelu@cchmc.org

Received June 3, 2014; accepted for publication January 7, 2015; published Online First on February 23, 2015.

1066-5099/2015/$20.00/0

http://dx.doi.org/10.5966/sctm.2014-0107

ABSTRACT

The glial scar resulting from spinal cord injury is rich in chondroitin sulfate proteoglycan (CSPG), a formidable barrier to axonal regeneration. We explored the possibility of breaching that barrier by first examining the scar in a functional in vitro model. We found that embryonic stem cell-derived neural lineage cells (ESNLCs) with prominent expression of nerve glial antigen 2 (NG2) survived, passed through an increasingly inhibitory gradient of CSPG, and expressed matrix metalloproteinase 9 (MMP-9) at the appropriate stage of their development. Outgrowth of axons from ESNLCs followed because the migrating cells sculpted pathways in which CSPG was degraded. The degradative mechanism involved MMP-9 but not MMP-2. To confirm these results in vivo, we transplanted ESNLCs directly into the cavity of a contused spinal cord 9 days after injury. A week later, ESNLCs survived and were expressing both NG2 and MMP-9. Their axons had grown through long distances (>10 mm), although they preferred to traverse white rather than gray matter. These data are consistent with the concept that expression of inhibitory CSPG within the injury scar is an important impediment to regeneration but that NG2+ progenitors derived from ESNLCs can modify the microenvironment to allow axons to grow through the barrier. This beneficial action may be partly due to developmental expression of MMP-9. We conclude that it might eventually be possible to encourage axonal regeneration in the human spinal cord by transplanting ESNLCs or other cells that express NG2. STEM CELLS TRANSLATIONAL MEDICINE *2015;4:401–411*

INTRODUCTION

The injured adult spinal cord can regain limited function, despite a well-formed glial scar and early syrinx formation. Proliferation of endogenous oligodendrocyte progenitors is one regenerative mechanism, but its role in long-term recovery is poorly understood. Moreover, our ideas about the expression of nerve glial antigen 2 (NG2), a chondroitin sulfate proteoglycan (CSPG), are in flux. It has long been thought that NG2 inhibits nervous system regeneration by contributing to glial scar formation [1, 2]. In 1994, Dou and Levine [3] first demonstrated that NG2 inhibits axon outgrowth in vitro. In 2003, Jones et al. [4] noted that axons appear to be closely associated with NG2 in chronically injured spinal cords.

After spinal cord injury and within the glial scar, the extracellular matrix contains several different CSPGs whose repulsive properties result largely from glycosaminoglycan (GAG) components attached to a protein backbone. As early as 72 hours after spinal cord injury (SCI), CSPG expression is sufficient to inhibit axonal outgrowth [4]. However, masking, disrupting, or avoiding expression of these specific inhibitory proteins enhances neurite regrowth and sprouting [5–12]. For example, immediately after dorsal column crush injury, intrathecal injection of a bacterial enzyme, chondroitinase ABC, cleaved GAG chains from the protein core, permitting axonal growth and partial functional recovery [9]. However, injecting the enzyme directly into injured tissue can cause bystander cell injury, elicit an inflammatory response, and promote some reformation of the inhibitory scar without long-distance axonal regrowth. Additionally, ablation of recruited endogenous astrocytic progenitors that contribute to the glial scar is detrimental to the neurotrophic support and prevention of furthered axonal loss [13].

Other factors that can support axonal regeneration include elevating cAMP levels, expressing neurotrophic factors, inhibiting epidermal growth factor receptor, inhibiting ρ, creating supportive biomaterial bridges, and transplanting nerve cell progenitors [14–27]. Inevitably, a combination of strategies that target both intrinsic and extrinsic causes of regeneration failure may be required, not only for multilineage cell survival

and repair but also for axonal regrowth [12, 28–32]. However, few studies have looked beyond the acute injury period, when the glial scar is fully developed [33–38]. Remarkable long-distance axonal growth was achieved in transected rat spinal cords receiving delayed transplantation of neural stem cells 2 weeks after injury [39]. The intrinsic properties of immature neural cells, combined with growth factors and scaffolds, demonstrate potential for new axonal growth, even after delayed periods of time in which the glial scar is well formed.

We addressed this issue by transplanting embryonic stem cell-derived neural lineage cells (ESNLCs) 9 days after injury and examining the spinal cord a week later. Neurally induced embryonic stem cells are model systems for microenvironmental studies because they are capable of remyelination in the diseased spinal cord when guided toward the oligodendroglial lineage [40, 41]. They can also be genetically engineered to express green fluorescent protein. We first examined various stages of embryonic stem (ES) cells along the neural lineage in a functional in vitro model of the glial scar. We then transplanted neurally induced ES cells into the spinal cord, hypothesizing that such cells could support axonal outgrowth even after the syrinx had filled with fluid and a glial scar had formed. Our results provide the first evidence that cellular support for axonal outgrowth through the glial scar may be a property of the NG2+ cell, challenging the idea that NG2 expression is always inhibitory. The mechanism involves a metalloproteinase, matrix metalloproteinase 9 (MMP-9). Our study opens the door to new treatment strategies by suggesting that various cell types expressing NG2 might stimulate axonal growth even after the acute phase of SCI is over.

Materials and Methods

Cell Culture

B5 (strain 129SVJ; A. Nagy, University of Toronto, Toronto, Canada) [42] and Rosa 26 (from E.J. Robertson) male murine ES cell lines were maintained at low passage (<25 passages in our laboratory) with normal karyotypes [40]. R26 ES cells or B5 ES cells were differentiated using the 4−/4+ retinoic acid protocol by withdrawing leukemia inhibitory factor (Chemicon, Temecula, CA, http://www.chemicon.com) on day 0. They were cultured in Neurobasal A (Invitrogen, Carlsbad, CA, http://www.invitrogen.com) containing B27, L-glutamine, and penicillin/streptomycin [40, 43, 44]. The cells were collected via centrifugation and resuspended in culture medium. To identify transplanted B5 ES cells, continuous expression of enhanced green fluorescent protein (GFP) was optimized in the clonal B5 ES cell line by maintaining G418 (gentamicin; 500 μg/ml) in the culture medium during passage of undifferentiated ES cells prior to neural induction, culture, and transplantation [42]. Rosa 26 ES cells lack GFP expression and instead were prelabeled with Hoechst 33342 nuclear labeling as a marker to identify these cells after transplantation in all replicated experiments [32, 40, 43]. For culture experiments, cells were cultured at a density of 5×10^5/coverslip on a substrate of poly-L-lysine, nitrocellulose, and an inhibitory spot gradient comprised of 20 μg/ml laminin (Biomedical Technologies, Inc., Wardhill, MA, http://www.btiinc.com) and 0.7 mg/ml aggrecan (Sigma-Aldrich, St. Louis, MO, http://www.sigmaaldrich.com). Polylysine-coated glass coverslips were coated with a dropped spot of the 2-μl solution of aggrecan/laminin. This method creates an outermost inhibitory rim. Spotted coverslips were allowed to dry at 37°C for at least 5 hours prior to use in cell culture/plating experiments) [45]. Cells were cultured for 3 hours, 24 hours, 3 days, or 5 days and then fixed in 2% paraformaldehyde (PFA) for 1 hour and then 4% PFA for 30 minutes. Dorsal root ganglion (DRG) control cells were collected from adult female Sprague-Dawley rats (Zivic-Miller, Portersville, PA, www.zivic-miller.com), dissociated in dispase/collagenase, and resuspended in Neurobasal A containing B27, L-glutamine, and penicillin/streptomycin. DRGs were cultured at 1,000 cells per coverslip on the laminin/aggrecan gradient for 5 days before a 30-minute 4% PFA fixation and immunostaining identical to that used for the ES cells.

Spinal Cord Injury

Forty-four adult Long Evans female rats (275 ± 25 g of body weight; Simonsen Laboratories, Gilroy, CA, http://www.simlab.com/) were anesthetized with ketamine and Domitor (100 and 1 mg/ml, respectively, intraperitoneally). A laminectomy was performed at level T9−10, and a contusion injury was produced by dropping a 10-g weight (2.5 mm in diameter) onto the dorsal surface of the cord from a height of 25 mm (New York University weight-drop injury device). During all surgical procedures and 2 hours after the contusion injury, thermoregulation (36.5°C ± 0.5°C) was maintained with a thermostatically regulated heating pad (Versa-Therm 2156; Cole-Parmer, Chicago, IL, http://www.coleparmer.com) and with convection heat from a rectal temperature-based heating lamp, using a closed loop. Anesthesia was reversed by Antisedan (0.06 ml subcutaneously; Pfizer, New York, NY, http://www.pfizer.com). Autothermoregulation was normal 2 hours after reversal [40]. Cyclosporine (10 mg/kg) was administered daily, beginning 1 day before transplantation.

Transplantation

Nine days after SCI, a prominent, circumscribed glial scar was visible around the contusion injury cavity. In our preliminary experiments, we transplanted 1 million mouse ES-derived neural progenitor cells (both cell lines prelabeled with Hoechst 33342) or ES cell induction medium (vehicle control) directly into the cyst at the injury epicenter (n = 5 for each group). We then performed time-independent replications of transplantation studies representing these two groups: ES-derived neural progenitors (n = 14) and vehicle control (n = 10). To control for possible cellular uptake of GFP from dead transplanted cells, we performed additional control experiments: transplantation of (a) frozen, dead ES cells (n = 5) and (b) GFP+ fibroblasts (n = 5). Transplantations were performed stereotaxically (Kopf models 5000 and 900; David Kopf Instruments, Tujunga, CA, http://www.kopfinstruments.com) into the center of the injury cyst at the T9 level over a 5-minute period (total volume = 5 μl), using a 5-μl Hamilton syringe [43]. Animals were sacrificed 1 week after transplantation (16 days after SCI).

Animal Care

All surgical interventions and animal care were provided in accordance with the Laboratory Animal Welfare Act, the Guide for the Care and Use of Laboratory Animals, and the Guidelines and Policies for Rodent Survival Surgery provided by the Animal Studies Committees of Washington University School of Medicine in St. Louis and Johns Hopkins University School of Medicine. The studies were performed at both institutions, using our published protocols [40, 43].

Immunohistochemistry

Whole animal fixation was completed by transcardial injection of buffered paraformaldehyde solution. The spinal cord was removed, frozen at −40°C in isopentane, stored at −70°C, and sectioned (14 μm) while frozen. Immunohistochemistry was performed as previously detailed [40].

For in vitro experiments, immunostaining was completed in phosphate-buffered saline containing 5% nerve growth serum, 0.1% bovine serum albumin, and 0.1% Triton. Anti CS-56 (Sigma-Aldrich; 1:100; used to visualize proteoglycan in the gradient) was biotinylated (Molecular Probes, Eugene, OR, http://probes.invitrogen.com; 1:500) and visualized with Texas Red-conjugated streptavidin (Chemicon; 1:200). Cells were visualized with primary antibodies against β-tubulin (Sigma-Aldrich; 1:400), nestin 130 rabbit polyclonal (gift from R.D.G. McKay, Bethesda, MD, 1:1,000), microtubule-associated protein 2 (MAP2) mouse IgG (Chemicon; 1:100), NG2 rabbit polyclonal (Chemicon; 1:1,000), A2B5 mouse IgM (Boehringer Mannheim, Mannheim, Germany, http://www.boehringer.com; 1:200), O4 mouse IgM (Developmental Studies Hybridoma Bank [DSHB], Iowa City, IA, http://dshb.biology.uiowa.edu; 1:50), glial fibrillary acidic protein (GFAP) rabbit polyclonal (DiaSorin, Varese, Italy, http://www.diasorin.com; 1:4), MMP-9 (rabbit, 1:1,000; Sigma-Aldrich), and Hoechst 33342 (Molecular Probes; 1:200) counterstain. Secondary antibodies included Molecular Probes Oregon Green (Life Technologies, Rockville, MD, http://www.lifetech.com; 1:500) or goat-derived CY-3 (Chemicon; 1:300).

For in vivo experiments, primary antibodies against NeuN (Chemicon; mouse IgG, 1:300), MAP2 (Chemicon; mouse IgG, 1:40), glutamate (DiaSorin; mouse IgG, 1:2,000), γ-aminobutyric acid (GABA; Immunostar, Hudson, WI, http://www.immunostar.com; IgG rabbit polyclonal, 1:500), choline acetyltransferase (ChAT; Chemicon; rabbit polyclonal, 1:3,000), and vesicular acetylcholine transferase (Chemicon; 1:2,000), SMI 31 (Sternberger, Dedham, MA, http://antibody.biolegend.com); mouse IgG, 1:10,000), SMI-311 (Sternberger; mouse IgG/IgM, 1:10,000), NG2 (Chemicon; rabbit polyclonal, 1:1,000), anti-adenomatous polyposis coli (APC; Calbiochem, San Diego, CA, http://www.emdbiosciences.com; mouse IgG2, 1:200), nestin 130 (R.D.G. McKay, Bethesda, MD; rabbit polyclonal, gift from 1:1,000), MMP-9 (Sigma-Aldrich; rabbit, 1:1,000), GFAP (DiaSorin; rabbit polyclonal, 1:4), anti-mouse EEM-1 (D.I. Gottlieb, Washington University School of Medicine; hamster IgG, 1:10), anti-LeX/SSEA-1 (gift from S. Temple Albany Medical College, 1:200), anti-mouse embryonic membrane antigen (rat IgG hybridoma, 1:4; DSHB), anti-mouse M2 (C. Lagenaur, University of Pittsburgh; rat IgM, 1:4), anti-mouse Thy 1.2 (Serotec Ltd., Oxford, U.K., http://www.serotec.com; rat IgM, 1:1,000), CS-56 (Sigma-Aldrich; mouse IgM 1:200), CSPG (Chemicon; mouse IgM 1:100), smooth muscle actin (Sigma-Aldrich; mouse IgG 1:400), anti-GFP (Molecular Probes; rabbit IgG/Alexa 488, 1:500), anti-GFP (Molecular Probes; mouse 3E6, 1:1,000), Hoechst 33342 counterstain and secondary antibodies against goat-derived CY-3 (Chemicon; 1:300), goat-derived CY-5 (Chemicon; 1:300), goat-derived Alexa 488 (Chemicon; 1:300), goat-derived biotinylated anti-hamster (Chemicon; 1:200), and goat-derived CY-3 avidin (Chemicon; 1:300).

Quantification

We calculated respective immunopositive subpopulations of surviving ES cells using confocal microscopy (i.e., ChAT+ expression with double immunofluorescent expression of markers for ChAT and stem cell-derived GFP) by examining three longitudinal sections (14 μm); the first was centered at the middle of the cord, and the other two were 200 μm in either the dorsal or ventral direction (n = 15). This number was divided by the total number of GFP+ ES cells counted per section, and the results were averaged per rat. GFP+/SMI+ neurite outgrowth was quantified (modified from a previously described method) by attaching a 1-mm grid template to sequentially count each 1mm area examined [46]. This was done by placing a 1-mm boxed grid pattern over observed transplant/glial scar zones and then counting each box sequentially in rostral and caudal directions and in white versus gray matter areas. Each ES-derived neurite (GFP-tagged) traversing the 1-mm boxed grid was quantified. The two blinded technicians were not directly involved with the study's hypothesis. For each respective immunolabel quantified at the glial scar interface, at least two zones per section were examined (20−40 zones per label) and compared, using Student's t test (accepted p values were $<.05$ [*] and $<.01$ [**]). Zones of CSPG expression (transplant/glial scar interface), neurite penetration, and NG2 cell localization were counted, and CSPG expression was converted to a bitmap mode, appearing in black/white on Adobe Photoshop software. We examined areas enclosed by a 100-μm-diameter circle generated from Adobe Photoshop. These images were converted to a binary mode for high and low CSPG expression. Both areas were examined for neurite penetration and tabulated as such; if they were crossed by a GFP+/SMI+ neurite, they were counted as

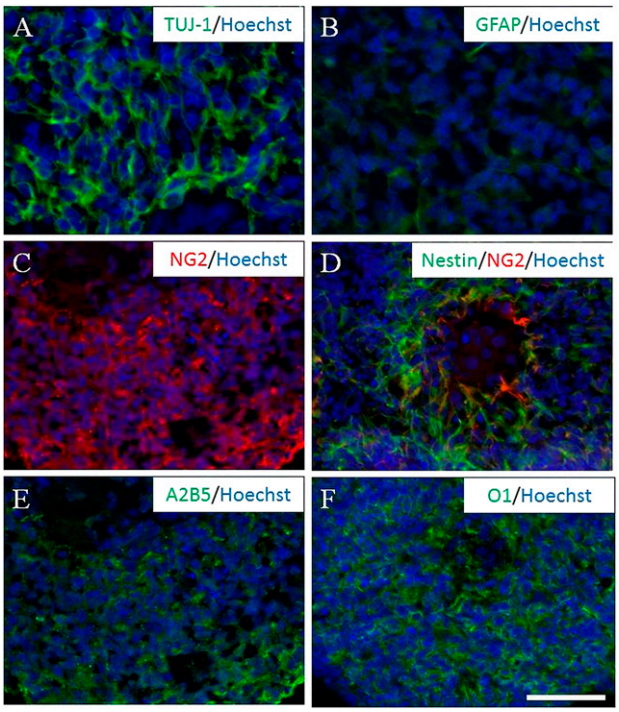

Figure 1. The 4−/4+ staged embryoid bodies (EBs) are immunoreactive for neural markers. **(A, B):** EB cells expressed positive for neural phenotypes, including neuronal (anti-TUJ-1 **[A]**) and astrocytic (anti-GFAP **[B]**) expression. **(C, D):**The majority of EB cells demonstrated early tripotential neural progenitor predominance, positive for oligodendroglial (anti-NG2, red **[C]**) and neural (anti-nestin, green; anti-NG2, red **[D]**) precursors. **(E, F):** However, other stages of oligodendroglial showed differentiation as well (anti-A2B5 **[E]** and anti-O1 **[F]**). Nuclei were counterstained with Hoechst 33342 (blue). Scale bar = 50 μm. Abbreviations: GFAP, glial fibrillary acidic protein; NG2, nerve glial antigen 2.

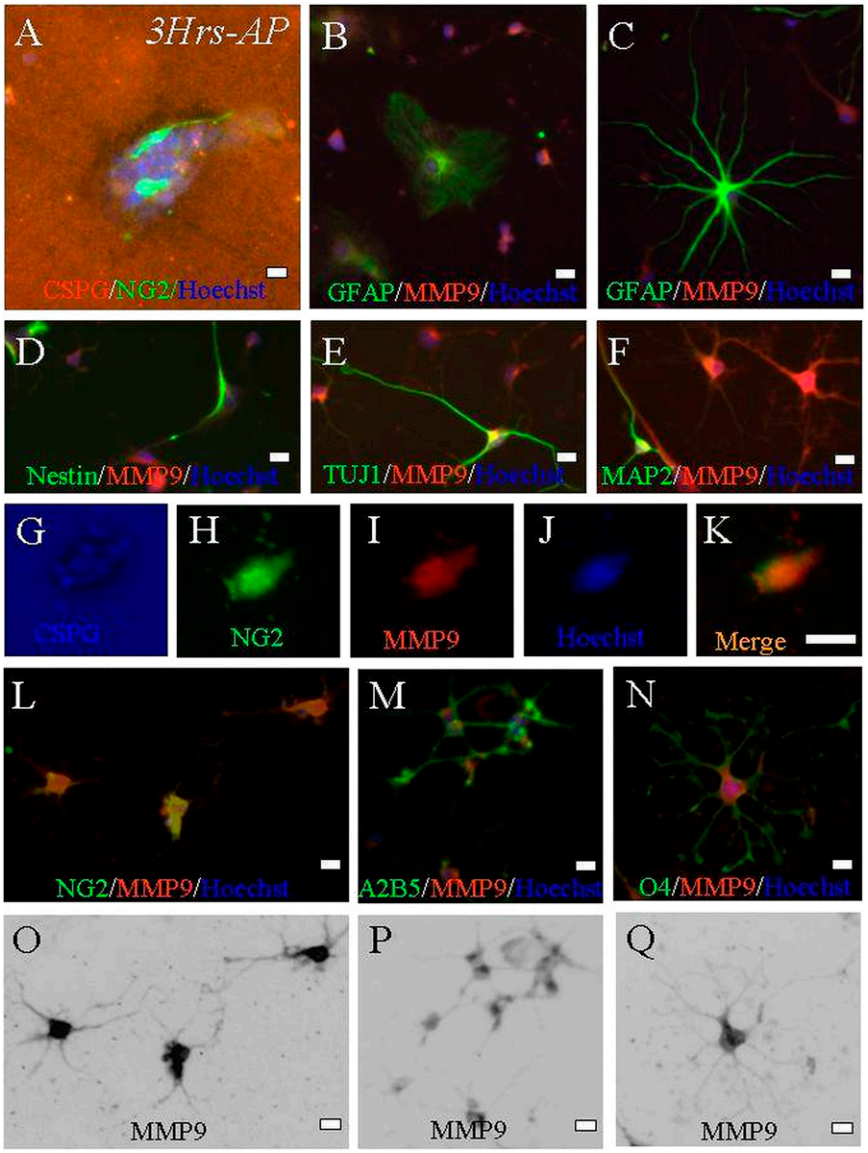

Figure 2. Embryonic stem (ES) cell-derived progenitors that can remodel CSPG express early glial characteristics when cultured on a monolayer of aggrecan. **(A):** Three hours after partially dissociated 4−/4+ staged neural-induced embryoid bodies were plated (CS-56, red), a percentage of ES cells survived and displayed early NG2+ expression (indicated by coexpression of NG2 and Hoechst nuclear counterstain; NG2, green; Hoechst nuclear label, blue). **(B–Q):** After 5 days of culture, differential immunostaining for neural phenotypes demonstrated colocalized expression of MMP-9 and NG2. Occasionally, some cells positive for GFAP (type I **[B]** and type II astrocytes **[C]**) and neuronal markers (nestin **[D]**, TUJ1 **[E]**, and MAP2 **[F]**) weakly expressed MMP-9 as well, but they were a small fraction of total MMP-9 cells. Stronger MMP-9 expression was evident in oligodendroglial cells at the stage when they strongly expressed NG2+ (two different cells are represented by **[G–K]** and **[L]**). **(M, N):** A diffuse, high level of MMP-9 expression that was more dense in cells coexpressing NG2+ than cells expressing the A2B5 or O4 phenotype (**[M]** and **[N]**, respectively). **(O–Q):** Inverted black/white-coded images of original photomicrographs. Scale bars = 10 μm. Abbreviations: CSPG, chondroitin sulfate proteoglycan; GFAP, glial fibrillary acidic protein; Hrs, hours; MMP9, matrix metalloproteinase 9; NG2, nerve glial antigen 2.

penetrated zones. The 100-μm circles enclosing either CSPG alone or CSPG penetrated by GFP+/SMI+ neurites were counted as zones with associated NG2+ or MMP-9+ cells if GFP cells were labeled with both NG2+ and MMP-9+. We evaluated long distance GFP+ axon outgrowth with the same blinded semiautomated quantification method described above; however, we only included processes that are observed extending greater than 2 mm from the cyst epicenter and outside the SCI cyst/scar barrier. Data comparing gray versus white matter long-distance outgrowth were evaluated for statistical significance with a repeated measures analysis of variance (Tukey's test, n = 5 rats). Five or six longitudinal sections spanning the graft were analyzed per animal.

In vitro studies were quantified by collecting black and white photomicrographs with a Leitz Orthoplan 2 fluorescence microscope attached to an Optronics digital camera and operated by Magnafire software. Seven images of CS-56 immunostaining (representing CSPGs) were randomly collected: six regions on the spot's rim and one in the spot's center. In these images, black represented blank areas (areas of digestion). The grayscale of the images was then inverted in Adobe Photoshop so the black areas

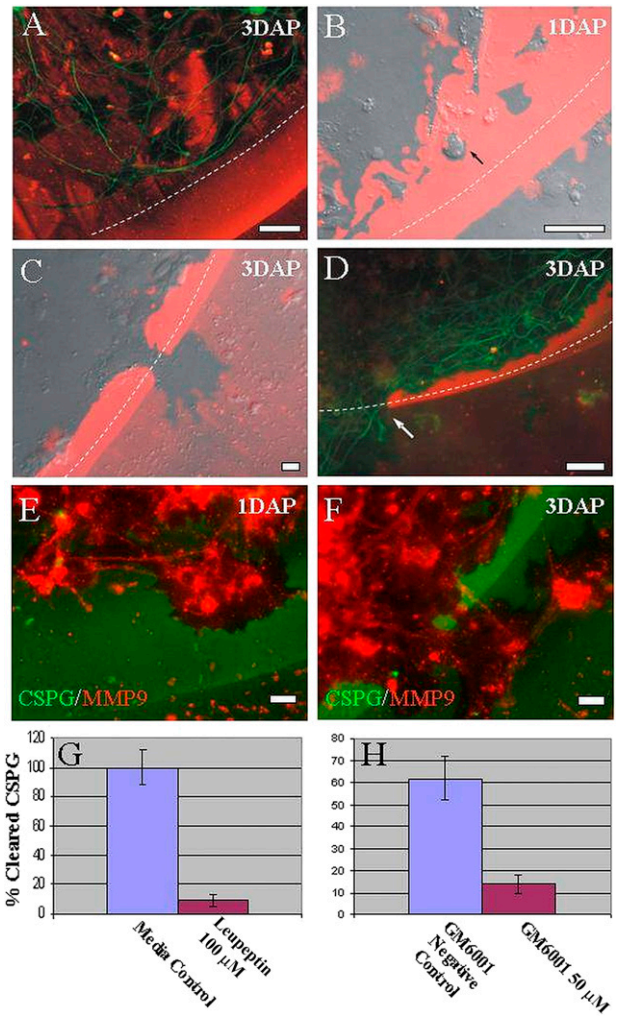

Figure 3. Embryonic stem (ES)-derived neural progenitors remodeled CSPG barriers in vitro (1–3 DAP) in our CSPG spot gradient model. When plated for longer than 3 hours as seen in Figure 2A, NG2 cells were capable of migrating through the most inhibitory rim at 1–3 days after plating. **(A):** Photomicrograph of DRG neurites (β-tubulin, green) inhibited by the edge of the CSPG gradient (CS-56, red). **(B, C):** Merged DIC and epifluorescence images of CSPG spot gradient with plated ES cell-derived progenitors (green fluorescent protein [GFP], green; CS-56, red). **(B):** ES cell-derived progenitor (black arrow) migrating through the CSPG spot gradient, demonstrating proteoglycan digestion (zones free of CSPG). **(C):** Breakthrough zone debrided of CSPG, where axons would subsequently grow across the CSPG spot gradient barrier. **(D):** ES cell-derived neural processes crossing the inhibitory CSPG spot gradient (β-tubulin, green; CS-56, red; white arrow indicates β-tubulin-positive process crossing CSPG-free zone of the spot gradient). **(E, F):** ES cell-derived neural progenitors 24–72 hours after plating in a CSPG spot gradient. ES cell-derived progenitors (GFP, green) exhibiting high MMP-9 expression (CS-56, red) associated with zones of CSPG removal. **(G, H):** Graph illustrates percentage of pixel area assigned to the absence of CS-56 epifluorescence as a function of values in untreated control, untreated control (ES cell-derived neural progenitor cultures), leupeptin (100 μM, specific inhibitor of MMP-9), GM6001 (50 μM, negative control), and GM6001 (50 μm, general inhibitor of MMP-9). Student's t test ($p < .05$) was used. Scale bars = 10 μm. Abbreviations: CSPG, chondroitin sulfate proteoglycan; DAP, days after plating; MMP9, matrix metalloproteinase 9.

became white for analysis. The inverted images were quantified using Metamorph software. Areas of digestion (number of white pixels) were presented as a percentage of those in the control cultures (totaled white pixels set as the 100% threshold).

Results

ES Cells Preferentially Differentiate to an Oligodendroglial Lineage on Aggrecan Monolayers

Genetically tagged B5 ES cells capable of overexpressing GFP and Rosa 26 ES cells that were not genetically tagged were exposed to retinoic acid following the 4−/4+ neural induction protocol [44]. Embryoid bodies—aggregates of neurally induced cells seen 8 days after the leukemia inhibitory factor was removed—were evaluated for neural phenotypic markers TUJ-1 and GFAP (Fig. 1A, 1B). Additionally, they were evaluated for neural precursor expression patterns (NG2, nestin, A2B5, and O1; Fig. 1C–1F) prior to culture and transplantation experiments. NG2+ expression occurred in 43% ± 2% (Fig. 1). Our previous work identified these early cells as tripotential neural progenitors (capable of differentiating into neurons, astrocytes, or oligodendrocytes) [40, 43, 47]. When 4−/4+ tripotential progenitors were plated as embryoid bodies on aggrecan monolayers, we observed glial predominance (3 hours to 3 days after plating), most being immunopositive for the NG2 marker (Fig. 2A). Five days after plating, only two populations survived on the dense aggrecan monolayers. The first was a limited population of GFAP-expressing cells that were in the same position as when plated on day 0. The second population did not immunoreact to GFAP, and the cells expressed NG2 and had a halo around them, suggesting they had migrated by degrading local CSPG (Fig. 2B–2K).

Penetration of the Inhibitory Rim During Migration on the Glial Scar Spot Gradient

Our second set of experiments involved a functional inhibitory model of the glial scar in vitro. As outlined by Tom et al. [48], we questioned the glial scar's inhibitory action on the 4−/4+ ES cells isolated against a gradient of aggrecan. Our main questions were:

- Is there a subpopulation of ES cell-derived cells that promotes CSPG breakdown rather than being reactive and promoting glial scar formation?
- Do newly formed axons have the intrinsic ability to respond to a harsh gradient of aggrecan and penetrate the inhibitory rim?

To answer these questions, we cultured ES-derived neural progenitors on a gradient of inhibitory substrates—a very potent in vitro model of proteoglycan-mediated inhibition [48]. Toward the outer edge of the gradient, a distinct rim of high aggrecan concentration and low laminin concentration inhibits all cellular growth, and normal neuronal processes of adult DRGs and all other cell types from ganglia (e.g., satellite cells) are unable to cross this barrier (Fig. 3A). When we cultured ESNLCs on this gradient, we noted amoeboid cells that digested the aggrecan within the gradient, even at the most inhibitory peripheral regions (Fig. 3B). In discrete regions of the inhibitory rim, those ES cell-derived cells, which were positive for NG2, digested their way completely through to the outside (Fig. 3C), even in the absence of neurons at the outer rim. Further staining revealed that β-tubulin-positive processes of other ES-derived neural progenitors were

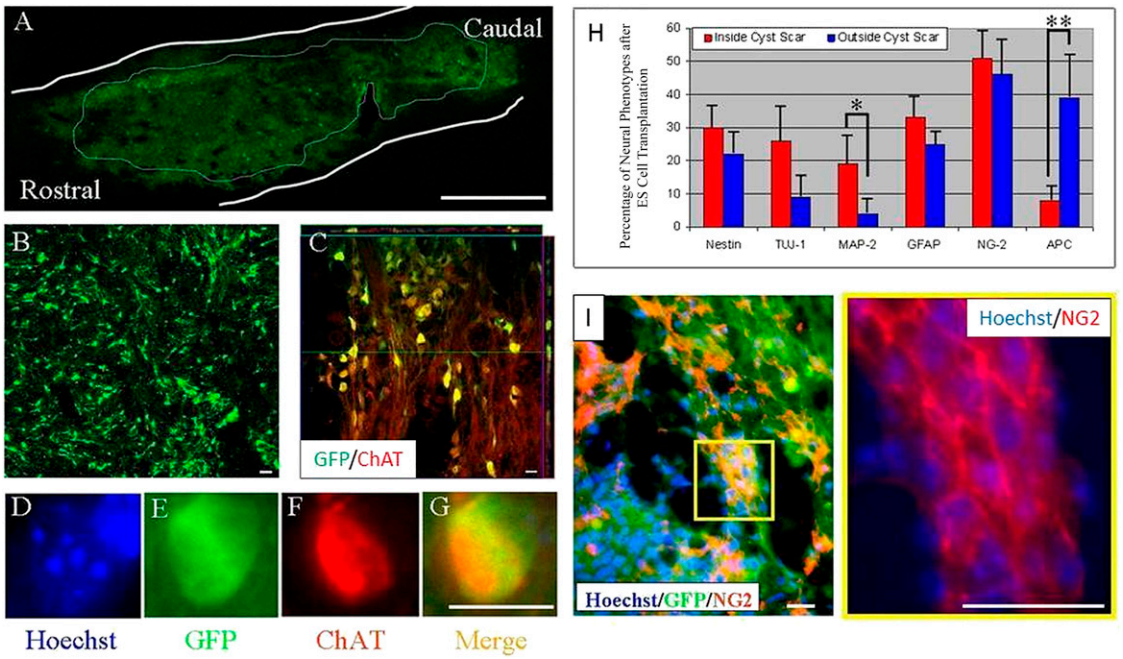

Figure 4. ES cell-derived neural progenitors induced using the 4−/4+ retinoic acid method [40, 43, 44] and transplanted into an injury-induced cyst differentiated into central nervous system-type neurons. **(A, B):** Transplanted ES cells expressed GFP within the center of the transplant. **(C):** One week after transplantation, ES cell-derived cells (green) had differentiated into neurons displaying ChAT (red) immunoreactivity (yellow indicates double labeling with GFP (green) and ChAT (red)). Orthogonal views of this image are outlined in green and red and are represented within the confocal image with their respective lines. **(D–G):** Hoechst nuclear counterstain (***D***, blue) identifies another transplanted ES cell (green **[E]**) that expressed GFP (green **[E]**) and ChAT (**[F]**, red; **[G]**, merge). Scale bars = 1 mm **(A)**, 10 μm. **(B–G)**. Differentiation of transplanted ES cells within the inhibitory microenvironment of the CSPG scar. **(H):** Percentage quantification of neural phenotypes inside and outside the cyst scar. **(I):** Photomicrograph illustrating that a majority of GFP+ cells that migrated out of the cavity were immunopositive for NG2. Yellow box inset from **(I)** shows individual NG2 labeling at higher magnification. Student's *t* test was used. $*$, $p < .05$; $**$, $p < .01$. Transplanted cells shown here were derived from the B5 GFP ES cell line. Scale bars = 20 μm **(I)**. Abbreviations: ChAT, choline acetyltransferase; ES, embryonic stem; GFAP, glial fibrillary acidic protein; GFP, green fluorescent protein; NG2, nerve glial antigen 2.

then able to cross the inhibitory rim by selectively growing through tunnels freed of aggrecan (Fig. 3D). This observation points to cellular penetration rather than initial axonal penetration as the predominant mechanism of passage.

MMP-9-Dependent Digestion of CSPG

We next questioned whether matrix metalloproteinases were involved in this functional clearance of CSPG in vitro. Indeed, we found that the digested areas (areas free of CSPG) coincided with MMP-9 expression (Fig. 3E, 3F). MMP-2, however, was not expressed. To test the proposed molecular mechanism of glial scar remodeling after ES cell-derived neural progenitors were plated, we applied leupeptin or GM6001 (specific and general MMP inhibitors, respectively). Whereas control or untreated cultures containing CSPG were fully digested, only 10%–15% of the territory was digested in the presence of the inhibitors (Fig. 3G, 3H). β-Tubulin-positive processes appeared to have crossed the barrier in areas where remodeling cells (ES cell-derived NG2+ cells) had already digested the aggrecan, suggesting that these cells might prepare the local environment for subsequent outgrowth of axons.

ES Cells Transplanted Within the Cyst Differentiate Into Neurons

To explore the fate of ES cell-derived neural cells in vivo, we first induced ES cells expressing GFP to form predominantly neural progenitors in culture [43]. Then we transplanted 1 million ES cells (Fig. 4A, 4B) or ES cell induction medium (vehicle) into the cavity of a lesion that we had created with a weight dropped 9 days previously. Injection directly into the syrinx allowed the ES cell-derived neural cells to fill most of the cavity without distorting the implantation site. Immunolabeling with GFP, Hoechst, and anti-mouse marker indicated that the transplanted cells remained within the injury cyst or just outside its perimeter (within one segment of the lesion's edge). This observation is consistent with our previous demonstration that migration of progenitor cells is limited and that the cells differentiate mostly into oligodendroglia or, in some cases, neurons or astrocytes (unpublished observations) [40, 43]. We observed no GFP expression in vehicle-transplanted animals.

One week after transplantation, many of the ES neural progenitors had differentiated into neuronal phenotypes akin to spinal cord cells, displaying GABA, glutamate, and ChAT immunoreactivity (Fig. 4C–4G). We identified neuronal differentiation using the NeuN immunolabel. Quantification of cells coexpressing the GFP and NeuN labels revealed that 12% $\pm$ 3% of the total number of surviving transplanted ES cells had neuronal properties and that 4% $\pm$ 4% of those neural cells displayed ChAT immunoreactivity.

Transplanted ES Cells Differentiate Into Oligodendrocyte Progenitors Within the Periscar Niche

At 1 week, transplanted cells located within the inhibitory microenvironment of the cystic scar (GFAP 33% $\pm$ 6%, NG2 51% $\pm$ 8%, and APC 8% $\pm$ 2%) or outside the scar (GFAP 25% $\pm$ 4%, NG2 46% $\pm$ 5%, and APC 39% $\pm$ 7%) had a glial phenotype. Various

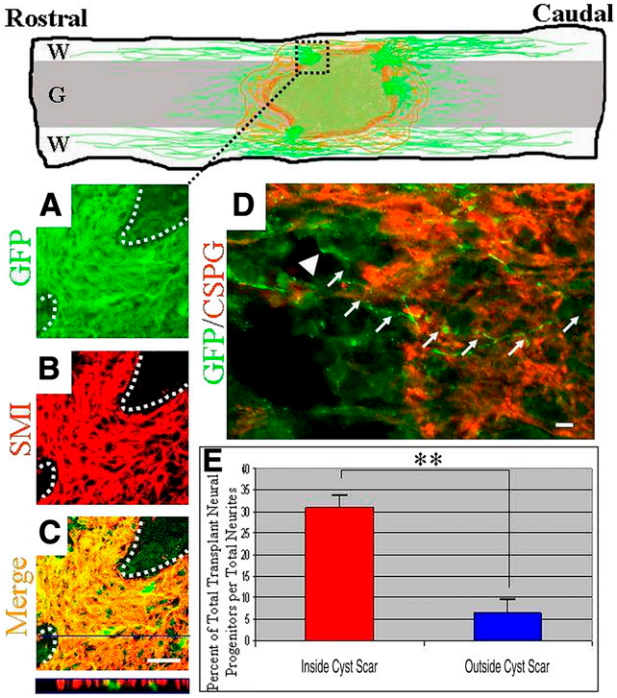

Figure 5. Transplanted embryonic stem (ES) cell-derived neurons extended axons in both rostral and caudal directions. **(A–C):** Reconstructed confocal micrographs demonstrate process profiles (GFP **[A]**) exhibiting the immunoreactivity (neurofilament **[B]** and merge **[C]**) of axons traversing the cyst glial scar (white dotted lines demarcate cyst barrier). **(C):** Merged view (orthogonal view outlined in blue is representative of demarcated blue line) demonstrates relatively few cells and numerous axons within this spatial pattern of robust outgrowth. **(D):** A GFP+ neuron extended its neurite (white arrows; white arrowhead represents neuronal cell body) through a relatively less dense CSPG zone, whereas it remained within the cyst cavity/transplantation site (GFP, green; CSPG, red). **(E):** Quantification of the number of GFP/Hoechst+ ES cell-derived cells relative to the number of GFP+ neurites within a 1-mm measurement box, comparing the inside and outside of the cyst cavity. The percentage is expressed in relation to the total number of axonal processes. Student's *t* test was used. $*$, $p < .05$; $**$, $p < .01$. Transplanted cells shown here were derived from the B5 GFP ES cell line. Scale bars = 10 μm **(A–C)**, 20 μm **(D)**. Abbreviations: CSPG, chondroitin sulfate proteoglycan; G, gray matter; GFP, green fluorescent protein; W, white matter.

stages of oligodendroglial development were seen. In agreement with earlier observations, greater neuronal expression was observed inside (nestin 30% $\pm$ 4%, TUJ-1 26% $\pm$ 7%, and MAP2 19% $\pm$ 8%) than outside (nestin 22% $\pm$ 9%, TUJ-1 9% $\pm$ 5%, and MAP2 4% $\pm$ 4%) the cyst scar (Fig. 4H, 4I).

Transplanted NG2+ ES Cells Associate With Axonal Penetration of the Glial Scar

We observed robust axonal outgrowth in distinct patterns penetrating through the well-developed scar. GFP+ processes elongated through zones of high CSPG expression within the scar and in both gray and white matter (supplemental online Fig. 1). On closer examination, it was evident that the axons preferred to elongate through areas with less dense CSPG expression (i.e., inhibitory areas that had been rendered permissive but were immediately adjacent to zones of high CSPG expression; supplemental online Fig. 1). We questioned whether axons outside the initial transplant site would correlate with the overall pattern of CSPG immunoreactivity per lesion. However, in this gross observation test, we were unable to demonstrate that the number of GFP+ neurites 2 mm from the epicenter (white or gray matter) or with the maximal length of neurite outgrowth (supplemental online Fig. 1, inset table) is associated with variations in CSPG expression.

Double labeling with antibodies to neurofilaments (SMI), microtubules (TUJ-1), or glial markers identified the processes extending >1 mm outside the cellular graft as axons and not processes of glial cells (Fig. 5A–5C; TUJ-1and GFAP data not shown). Axons that grew out from the transplanted cells projected through the glial scar in zones where CSPG concentrations may appear more permissive (Fig. 5D).

We could not determine which subclass of ES cell-derived neurons produced axons. Despite scar penetrance, it was unclear whether the axons themselves were initially derived from neurons within the cyst or extended from neurons adjacent to the scar. We examined this issue by comparing the number of cell bodies that were double-labeled for endogenous GFP expression and Hoechst nuclear labeling at two locations: 0.5 mm inside the glial scar (within the cyst) and 0.5 mm outside the scar. Both locations were within the 1-mm grid we centered over CSPG zones rendered permissive and populated with numerous axonal profiles. We examined the total number of immunopositive cell bodies within these respective locales and compared that with the overall number of processes traversing the glial scar throughout the 1-mm grid. This percentage of immunopositive neural cells per total neurites inside the cyst scar (31% $\pm$ 4%) compared with outside the scar (6.5% $\pm$ 2%) clearly indicated that, after a 1-week survival, long-distance neurites were derived predominantly from neurons within the cyst rather than from neurons located just outside the cyst (Fig. 5E). Therefore, transplanted neurons within the cyst/transplant location were the likely source of this long-distance neurite outgrowth.

We next examined whether the penetrated zones that were populated by NG2+ cells were capable of remodeling the glial scar, which had occurred in our functional in vitro modeling experiments. We found NG2+ cells concentrated within these zones concomitantly populated by an abundance of GFP+ neurites just within and outside the cyst scar barrier. When we compared zones of NG2+ cells with regions of high or low CSPG that also contained GFP+ processes, we found a strong correlation between axonal outgrowth and NG2+ cell activity in the general vicinity of CSPG+ areas of the cyst scar (Fig. 6). Examining the distribution of MMP-9 expression in the same zones, we found distinct labeling at the boundary of the cyst scar (Fig. 6D, demarcated by yellow dashed lines) and within the ES cell graft. By counting the number of zones of CSPG that had been penetrated by axons at these locales, we observed metalloproteinase activity, in agreement with our in vitro data. Confocal microscopy showed that 43% $\pm$ 4% of the transplanted cells in the inhibitory CSPG-cyst scar were positive for MMP-9 (Fig. 6E–6G). Three-dimensional reconstruction at single-cell resolution demonstrated a large area of MMP-9 expression (Fig. 6H, 6I) rather than areas limited to oligodendrocyte bodies and processes. These in vivo experiments showed that MMP-9 is a critical component of the remodeling activity of ES cells in microenvironments that normally inhibit axonal outgrowth.

Preferential Axonal Outgrowth in White Matter Rather Than Gray Matter

Using confocal microscopy, we measured the outgrowth of neurites in 1-mm segments 1.5 cm rostral and caudal to the epicenter.

A

NG2 Labeled ES Cells Associate with Axon Penetrated Zones			
Animal ID#	# of high CSPG zones	# of high CSPG zones penetrated by gfp+ neurites	# of penetrated zones with NG2 labeled ES cells
J18A5	6	5	5
S19A5	8	6	6
S19A6	10	8	7
S19A8	4	4	4
S19A9	7	4	6

B

MMP9 Labeled ES Cells Associate with Axon Penetrated Zones			
Animal ID#	# of high CSPG zones	# of high CSPG zones penetrated by gfp+ neurites	# of penetrated zones with MMP9 labeled ES cells
J18A5	6	5	5
S19A5	8	6	6
S19A6	10	8	7
S19A8	4	4	4
S19A9	7	4	6

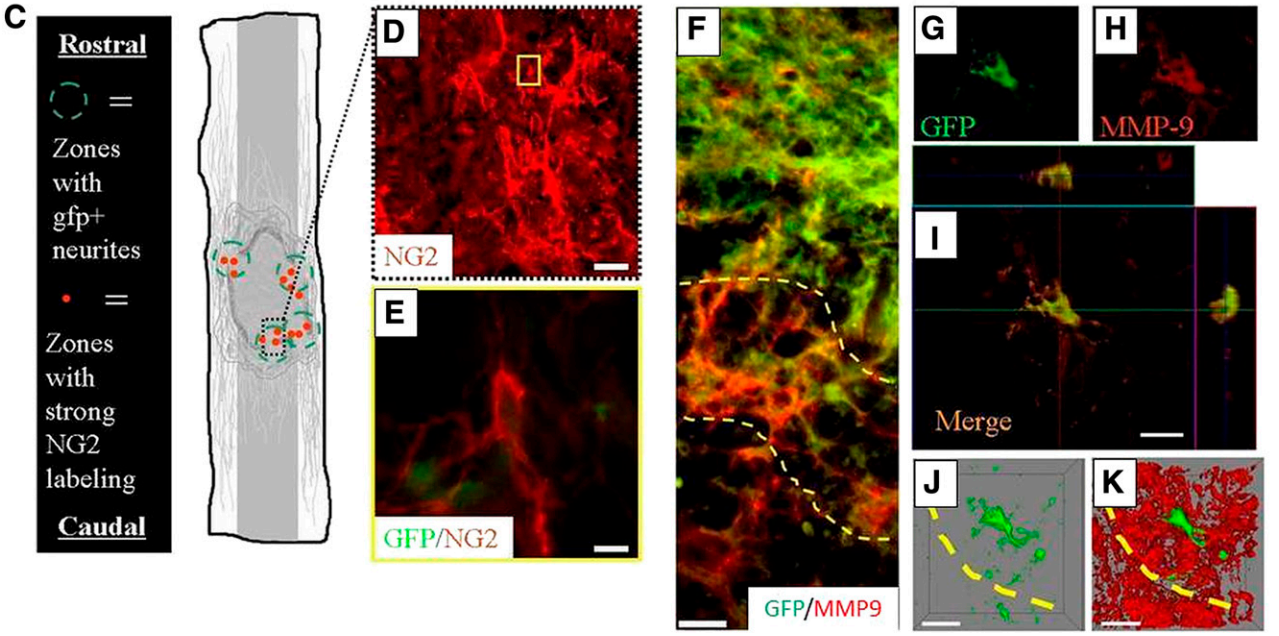

Figure 6. After being transplanted into the contused adult rat spinal cord, ES cells expressed NG2 in zones of high CSPG expression. **(A, B):** The cavity displayed intense zones of the highest CSPG expression (as determined by consistent, low-power epifluorescent imaging), zones penetrated by axons, and zones infiltrated with transplanted ES cells showing NG2 immunoreactivity. **(C):** Schematic illustration of zones of high CSPG expression that contain NG2+ ES cells penetrated by axons (green dashed circles represent high CSPG zones penetrated by GFP+ neurites, and red solid dots indicate penetrated zones populated with numerous NG2 labeled cells). **(D):** Midpower image demonstrating strong NG2 expression located at the graft/cyst cavity border. **(E):** Image corresponding to yellow box inset in **(D)**, demonstrating an individual transplanted NG2+ cell colabeled with GFP passing through graft/cyst zones. Scale bars = 10 μm. ES-derived neural progenitors displayed MMP-9 immunoreactivity in zones of high CSPG expression after being transplanted into the contused adult rat spinal cord. Inset: The cavity displayed a profile similar to that of NG2+ labeled zones, demonstrating consistent labeling of MMP-9 where axons penetrated. **(F):** MMP-9 was expressed in diffuse patterns at the glial scar boundary (demarcated by dashed yellow lines; GFP, green; MMP-9, red). **(G, H):** A GFP+ transplanted ES cell (GFP, green **[G]**) colocalized with MMP-9 expression (CS-56, red **[H]**) at the graft/cyst cavity border (dashed yellow line). **(I):** Three-axis view of merged images represented in **(G)** and **(H)**. Orthogonal views of this image are outlined in green and red and are represented within the confocal image **(I)** with their respective lines. **(G, H):** Reconstructed three-dimensional images of the same transplanted ES cell-derived neural cells shown in **(J)** and **(K)**, demonstrating the extent of MMP-9 expression to a single cell in vivo. Transplanted cells shown here were derived from the B5 GFP ES cell line. Scale bars = 20 μm **(D)**, 10 μm **(E–I)**. Abbreviations: CSPG, chondroitin sulfate proteoglycan; ES, embryonic stem; gfp or GFP, green fluorescent protein; MMP9, matrix metalloproteinase 9; NG2, nerve glial antigen 2.

We observed a predilection for long-distance outgrowth into white rather than gray matter (Fig. 7A–7D). GFP+ growth cones were evident in white matter even 8 mm away from the lesion's edge, which was 10 mm from the injury epicenter (Fig. 7D, inset). Blinded counters detected significantly more neurites in white matter than in gray matter 2–6 mm from the epicenter (Fig. 7E). One week after transplantation, the longest axons extended more than 9 mm from the epicenter into rostral white matter.

Discussion

Our results promote a novel mechanism for axonal outgrowth from a well-developed cyst scar and at a delayed time point after traumatic SCI. We observed that neurally induced ES cells with remodeling activity digested through proteoglycans within an inhibitory spot gradient in vitro and through a cyst scar after contusion SCI, although CSPG expression indicated no overall change in glial scar size. Neural progenitors were capable of crossing the cyst scar, with a large population expressing glial characteristics, including a unique population of NG2+ cells that also had metalloproteinase activity. These cells were dependent on MMP-9, but not MMP-2, and their migration was followed by robust axonal outgrowth from other ESNLCs, both in vitro and in vivo. Axonal outgrowth was greater in white matter than in gray matter, including over the longest distance.

There are several reasons why newly derived axons might follow NG2+ cells whose surface is thought to be inhibitory [49]. For example, axons might prefer to regrow by following NG2+ cells across the CSPG barrier rather than by using them as a scaffold. However, Jones et al. [4] showed that the pattern of NG2 expression closely approximated that of regenerating fibers [14–27, 33–38, 50, 51], whereas Nishiyama's group [52] demonstrated

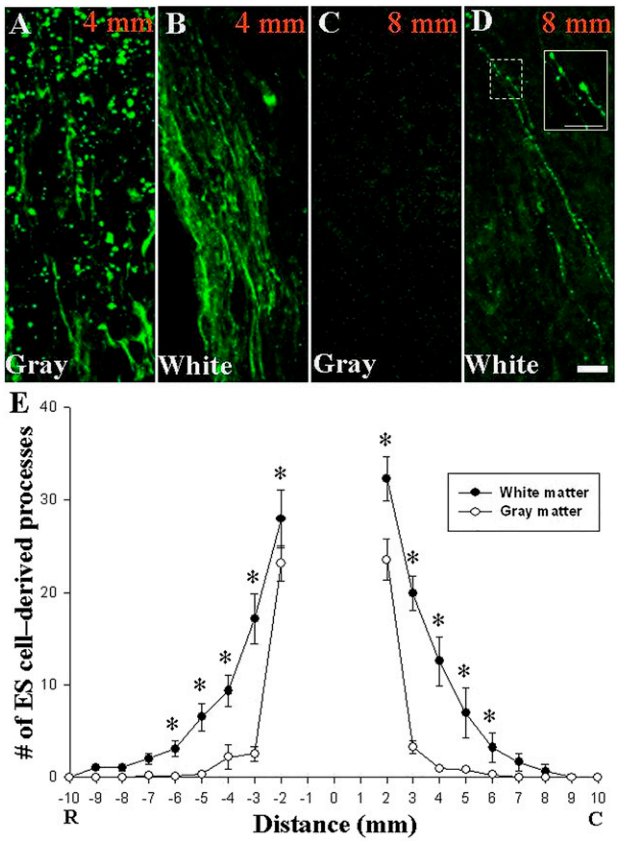

Figure 7. Neurite outgrowth indicated rapid growth through white matter in the injured adult rat spinal cord. **(A–D):** Confocal images of GFP-expressing ES cell-derived neurites (green) extending through gray **(A, C)** and white **(B, D)** matter at −4 mm **(A, B)** and −8 mm **(C, D)** rostral to the epicenter. One week after transplantation into a cavity caused by contusion injury, long-distance outgrowth was observed in white matter, whereas few processes were observed in gray matter beyond 4 mm. **(D):** Growth cone-like structures expressing GFP were apparent in white matter (white box inset demonstrates magnified field represented by dotted box. **(E):** Blinded quantification of GFP+ processes crossing each millimeter of cord demonstrated that neurites grew preferentially through white matter. $*$, $p < .001$ (repeated measures analysis of variance with Tukey's test, 2−6 mm in both rostral and caudal directions, white matter vs. gray matter; data represent means ± SEM, $n = 5$ rats; 5−6 longitudinal sections spanning the graft were analyzed per animal). Transplanted cells shown here were derived from the B5 GFP ES cell line. Scale bars = 100 μm **(A–D)**, 10 μm (inset in **[D]**). Abbreviations: C, caudal; R, rostral.

that NG2+ oligodendrocyte progenitors associated with axonal growth in hippocampal cocultures and callosal axons in vivo. These important findings may not contradict our hypothesis, because it is not possible to differentiate following from scaffolding in postmortem tissue from single time points after injury. Alternatively, the intrinsic nature of embryonic derived axons may represent immaturity with growth across chondroitin sulfate proteoglycans [53], suggestive of axonal elongation without regard to receptor based inhibition, for example, leukocyte common antigen-related phosphatase [54].

MMP-9, along with MMP-2 and -3, plays important roles in wound remodeling, cell migration, and neurite outgrowth after SCI [55]. Although endogenous cells in the injured spinal cord express MMP-9 early after injury [56], levels are insufficient to contribute to significant axonal regrowth, and MMP-2 expression predominates at 1 week [56]. Therefore, cellular expression of MMP-9 9 days after injury suggests ES cell-derived expression rather than an endogenous inflammatory response.

Taken together, our results suggest that the injured spinal cord has an MMP-9-dependent ability to remodel CSPG. This property came primarily from transplanted ES cell-derived progenitors that were positive for NG2. The evidence includes (a) the creation of CSPG-free tunnels in our in vitro CSPG spot gradient associated with ES cell-derived progenitor migration and was MMP-9 dependent; (b) our culture system was free of other cells such as macrophages and other non-neural cells known to produce MMP-9; (c) production of MMP-9 by non-neural cells is unlikely to play a substantial role in CSPG remodeling 9 days after contusion injury, because it occurs earlier in injured spinal cord models; (d) endogenous cells express MMP-2 at week 2, but MMP-2 inhibitors had no effect in our CSPG spot gradient [56], and (e) we used cyclosporine in our cultures, which deterred a macrophage response.

Our in vivo observations that ES cell-derived progenitors colabeled with NG2 and MMP-9 migrated across the CSPG barrier in the glial scar are in keeping with the observations of our in vitro CSPG spot gradient. Although we have not yet determined which subtypes of ES cell-derived NG2+ progenitor cells make MMP-9 in our systems, oligodendrocyte progenitors are known to express the proteinase early in central nervous system (CNS) oligogenesis [57–59]. Although it is possible that the active population of NG2+ ES cells shown here are early staged oligodendrocytes, we do not demonstrate in these studies that NG2 labeling is exclusive to a homogenous cell lineage. Additionally, our laboratory has recently published observations of CSPGs modulating NG2+ oligodendrocyte process extension and myelination but not differentiation through the tyrosine phosphatase σ receptor [60]. Whether CSPG affects the MMP-9 degradative mechanism of NG2+ cells is a topic for future experiments. Interestingly, ES-derived NG2+ cells capable of CSPG degradation with MMP-9 expression observed here may not, however, be capable at this stage of engaging in synaptic commitment unlike recently demonstrated reactive NG2+ cells up-regulated in injured host spinal cord tissue capable of entrapping dystrophic adult axons [61].

Robust expression of MMP-9 in and around the CSPG scar in our in vivo study was exclusive to ES cell-derived progenitors. We have not yet attempted to characterize the contribution of MMP-9 expression from endogenous NG2+ progenitors, which are known to proliferate at this phase of injury [62–65].

Previous studies suggest that MMPs derived from the axonal growth cone are also important for matrix remodeling and that they promote axonal regeneration in the peripheral nervous system [66]. Moreover, Duchossoy et al. [67] correlated gelatinase degradation of scar tissue in the injured spinal cord with ingrowing neurites. However, we did not see axons crossing areas of high CSPG, which suggests that release of MMP-9 by the axonal growth cone is not by itself sufficient to break down the formidable CSPG gradient barrier. Therefore, an important finding that differentiates our data is that delivery of MMP-9 from progenitor cells—rather than from axonal growth cones alone—is the primary mechanism for the scar remodeling that promotes robust axonal regeneration out of the cyst and into the injured spinal cord.

We do not believe our progenitor cells produced MMP-9 because they were tumorigenic (MMP-9 is also expressed when tumor cells migrate [68]). We evaluated this possibility by repeating our experiments with ES cell lines of low passage number (<25 passages) and different origins and obtained the same results as before. Moreover, all routine evaluations of karyotypes in our laboratory

have demonstrated euploid cell lines within this range of passage number (unpublished observations). Also, this study and our previous studies of transplanted ES cell-derived neural progenitors and those of many other groups have consistently demonstrated that these cells show normal growth contact inhibition (including self-limited cell proliferation and the absence of tissue overgrowth), normal patterns of cellular differentiation (i.e., absence of teratoma formation), and normal cell density. Finally, we observed selective MMP-9 expression in NG2+ cells and showed that degradation was dependent on MMP-9, but not MMP-2, which also argues against generalized transformation.

Conclusion

Our central findings are that delayed transplantation of ES cell-derived neural progenitors (a) produces NG2+ neural precursors that remodel the CSPG scar via an MMP-9-dependent mechanism; (b) extends axons over long distances at rates of >1 mm per day; and (c) regenerates with a preference for regrowth in white matter tracts. These events occurred 9 days after SCI, despite the development of a glial scar with prominent growth inhibition. We provide the first evidence that newly formed CNS neurons can grow axons through a well-formed injury-induced glial scar that produces CSPGs. Our data are consistent with the hypothesis that inhibitory CSPGs normally block axonal regeneration but that transplanted progenitor cells sculpt tunnels through the glial scar that are free of CSPG.

Acknowledgments

We are grateful to Drs. Hongxin Dong, Michael J. Howard, Andres Hurtado, Ashley Johnson, Aiwu Lu, Jared Miller, Martin Oudega, and Veronica Tom for technical expertise and critical discussions; Joan Bonnot and Monica Thigpen for excellent animal care; David Gottlieb for the EEM-1 antibody; Carl Lagenaur for the M2 antibody; Ron McKay for the Nestin 130 antibody; and Sally Temple for the LeX/SSEA-1 antibody. We acknowledge both Linda Sage and Avanti Vadivelu for editorial services and manuscript preparation. This work was supported by NIH National Institute of Neurological Disorders and Stroke (NINDS) Grants NS39577 and NS36265, the Christopher Reeve Paralysis Foundation, the International NTT Fund (to J.W.M.), and by NIH NINDS Grant NS25713 and a grant from the State of New York (to J.S.).

Author Contributions

S.V.: conception and design, provision of study material or patients, collection and/or assembly of data, data analysis and interpretation, manuscript writing, final approval of manuscript; T.J.S.: collection and/or assembly of data, final approval of manuscript; Y.Q. and S.L.: collection and/or assembly of data, data analysis and interpretation, final approval of manuscript; K.H.: provision of study material or patients, collection and/or assembly of data, data analysis and interpretation; Q.L.: data analysis and interpretation, final approval of manuscript; J.S.: conception and design, financial support, data analysis and interpretation, manuscript writing, final approval of manuscript; J.W.M.: conception and design, financial support, administrative support, provision of study material or patients, data analysis and interpretation, manuscript writing, final approval of manuscript.

Disclosure of Potential Conflicts of Interest

S.V. has uncompensated intellectual property rights. The other authors indicated no potential conflicts of interest.

References

1 Sellers DL, Maris DO, Horner PJ. Postinjury niches induce temporal shifts in progenitor fates to direct lesion repair after spinal cord injury. J Neurosci 2009;29:6722–6733.

2 Busch SA, Horn KP, Cuascut FX et al. Adult NG2+ cells are permissive to neurite outgrowth and stabilize sensory axons during macrophage-induced axonal dieback after spinal cord injury. J Neurosci 2010;30:255–265.

3 Dou CL, Levine JM. Inhibition of neurite growth by the NG2 chondroitin sulfate proteoglycan. J Neurosci 1994;14:7616–7628.

4 Jones LL, Sajed D, Tuszynski MH. Axonal regeneration through regions of chondroitin sulfate proteoglycan deposition after spinal cord injury: A balance of permissiveness and inhibition. J Neurosci 2003;23:9276–9288.

5 GrandPré T, Nakamura F, Vartanian T et al. Identification of the Nogo inhibitor of axon regeneration as a Reticulon protein. Nature 2000;403:439–444.

6 Davies SJ, Fitch MT, Memberg SP et al. Regeneration of adult axons in white matter tracts of the central nervous system. Nature 1997;390:680–683.

7 Davies SJ, Field PM, Raisman G. Embryonic tissue induces growth of adult axons from myelinated fiber tracts. Exp Neurol 1997;145:471–476.

8 Fouad K, Dietz V, Schwab ME. Improving axonal growth and functional recovery after experimental spinal cord injury by neutralizing myelin associated inhibitors. Brain Res Brain Res Rev 2001;36:204–212.

9 Bradbury EJ, Moon LD, Popat RJ et al. Chondroitinase ABC promotes functional recovery after spinal cord injury. Nature 2002;416:636–640.

10 Cafferty WB, Yang SH, Duffy PJ et al. Functional axonal regeneration through astrocytic scar genetically modified to digest chondroitin sulfate proteoglycans. J Neurosci 2007;27:2176–2185.

11 Houle JD, Tom VJ, Mayes D et al. Combining an autologous peripheral nervous system "bridge" and matrix modification by chondroitinase allows robust, functional regeneration beyond a hemisection lesion of the adult rat spinal cord. J Neurosci 2006;26:7405–7415.

12 Fouad K, Schnell L, Bunge MB et al. Combining Schwann cell bridges and olfactory-ensheathing glia grafts with chondroitinase promotes locomotor recovery after complete transection of the spinal cord. J Neurosci 2005;25:1169–1178.

13 Sabelström H, Stenudd M, Réu P et al. Resident neural stem cells restrict tissue damage and neuronal loss after spinal cord injury in mice. Science 2013;342:637–640.

14 Ankeny DP, McTigue DM, Jakeman LB. Bone marrow transplants provide tissue protection and directional guidance for axons after contusive spinal cord injury in rats. Exp Neurol 2004;190:17–31.

15 Nikulina E, Tidwell JL, Dai HN et al. The phosphodiesterase inhibitor rolipram delivered after a spinal cord lesion promotes axonal regeneration and functional recovery. Proc Natl Acad Sci USA 2004;101:8786–8790.

16 Ellezam B, Dubreuil C, Winton M et al. Inactivation of intracellular Rho to stimulate axon growth and regeneration. Prog Brain Res 2002;137:371–380.

17 Jin Y, Fischer I, Tessler A et al. Transplants of fibroblasts genetically modified to express BDNF promote axonal regeneration from supraspinal neurons following chronic spinal cord injury. Exp Neurol 2002;177:265–275.

18 Dergham P, Ellezam B, Essagian C et al. Rho signaling pathway targeted to promote spinal cord repair. J Neurosci 2002;22:6570–6577.

19 Qiu J, Cai D, Dai H et al. Spinal axon regeneration induced by elevation of cyclic AMP. Neuron 2002;34:895–903.

20 Wictorin K, Björklund A. Axon outgrowth from grafts of human embryonic spinal cord in the lesioned adult rat spinal cord. Neuroreport 1992;3:1045–1048.

21 Neumann S, Bradke F, Tessier-Lavigne M et al. Regeneration of sensory axons within the injured spinal cord induced by intraganglionic cAMP elevation. Neuron 2002;34:885–893.

22 Harper JM, Krishnan C, Darman JS et al. Axonal growth of embryonic stem cell-derived motoneurons in vitro and in motoneuron-injured

adult rats. Proc Natl Acad Sci USA 2004;101: 7123–7128.

23 Hill CE, Proschel C, Noble M et al. Acute transplantation of glial-restricted precursor cells into spinal cord contusion injuries: Survival, differentiation, and effects on lesion environment and axonal regeneration. Exp Neurol 2004;190:289–310.

24 Friedman JA, Windebank AJ, Moore MJ et al. Biodegradable polymer grafts for surgical repair of the injured spinal cord. Neurosurgery 2002;51:742–751.

25 McTigue DM, Horner PJ, Stokes BT et al. Neurotrophin-3 and brain-derived neurotrophic factor induce oligodendrocyte proliferation and myelination of regenerating axons in the contused adult rat spinal cord. J Neurosci 1998;18:5354–5365.

26 Koprivica V, Cho KS, Park JB et al. EGFR activation mediates inhibition of axon regeneration by myelin and chondroitin sulfate proteoglycans. Science 2005;310:106–110.

27 Nothias JM, Mitsui T, Shumsky JS et al. Combined effects of neurotrophin secreting transplants, exercise, and serotonergic drug challenge improve function in spinal rats. Neurorehabil Neural Repair 2005;19:296–312.

28 Lu P, Yang H, Jones LL et al. Combinatorial therapy with neurotrophins and cAMP promotes axonal regeneration beyond sites of spinal cord injury. J Neurosci 2004;24:6402–6409.

29 Pearse DD, Pereira FC, Marcillo AE et al. cAMP and Schwann cells promote axonal growth and functional recovery after spinal cord injury. Nat Med 2004;10:610–616.

30 Chau CH, Shum DK, Li H et al. Chondroitinase ABC enhances axonal regrowth through Schwann cell-seeded guidance channels after spinal cord injury. FASEB J 2004;18:194–196.

31 Steinmetz MP, Horn KP, Tom VJ et al. Chronic enhancement of the intrinsic growth capacity of sensory neurons combined with the degradation of inhibitory proteoglycans allows functional regeneration of sensory axons through the dorsal root entry zone in the mammalian spinal cord. J Neurosci 2005;25:8066–8076.

32 Vadivelu S, Platik MM, Choi L et al. Multigerm layer lineage central nervous system repair: Nerve and vascular cell generation by embryonic stem cells transplanted in the injured brain. J Neurosurg 2005;103:124–135.

33 Houle JD, Tessler A. Repair of chronic spinal cord injury. Exp Neurol 2003;182:247–260.

34 Reier PJ, Houle JD, Jakeman L et al. Transplantation of fetal spinal cord tissue into acute and chronic hemisection and contusion lesions of the adult rat spinal cord. Prog Brain Res 1988; 78:173–179.

35 Coumans JV, Lin TT, Dai HN et al. Axonal regeneration and functional recovery after complete spinal cord transection in rats by delayed treatment with transplants and neurotrophins. J Neurosci 2001;21:9334–9344.

36 Jin Y, Tessler A, Fischer I et al. Fibroblasts genetically modified to produce BDNF support regrowth of chronically injured serotonergic axons. Neurorehabil Neural Repair 2000;14:311–317.

37 Barakat DJ, Gaglani SM, Neravetla SR et al. Survival, integration, and axon growth support of glia transplanted into the chronically contused spinal cord. Cell Transplant 2005;14: 225–240.

38 Lu P, Jones LL, Tuszynski MH. Axon regeneration through scars and into sites of chronic spinal cord injury. Exp Neurol 2007;203:8–21.

39 Lu P, Wang Y, Graham L et al. Long-distance growth and connectivity of neural stem cells after severe spinal cord injury. Cell 2012;150:1264–1273.

40 Liu S, Qu Y, Stewart TJ et al. Embryonic stem cells differentiate into oligodendrocytes and myelinate in culture and after spinal cord transplantation. Proc Natl Acad Sci USA 2000; 97:6126–6131.

41 Keirstead HS, Nistor G, Bernal G et al. Human embryonic stem cell-derived oligodendrocyte progenitor cell transplants remyelinate and restore locomotion after spinal cord injury. J Neurosci 2005;25:4694–4705.

42 Hadjantonakis AK, Gertsenstein M, Ikawa M et al. Generating green fluorescent mice by germline transmission of green fluorescent ES cells. Mech Dev 1998;76:79–90.

43 McDonald JW, Liu XZ, Qu Y et al. Transplanted embryonic stem cells survive, differentiate and promote recovery in injured rat spinal cord. Nat Med 1999;5:1410–1412.

44 Bain G, Kitchens D, Yao M et al. Embryonic stem cells express neuronal properties in vitro. Dev Biol 1995;168:342–357.

45 Tom VJ, Steinmetz MP, Miller JH et al. Studies on the development and behavior of the dystrophic growth cone, the hallmark of regeneration failure, in an in vitro model of the glial scar and after spinal cord injury. J Neurosci 2004;24:6531–6539.

46 Dong H, Fazzaro A, Xiang C et al. Enhanced oligodendrocyte survival after spinal cord injury in Bax-deficient mice and mice with delayed Wallerian degeneration. J Neurosci 2003;23:8682–8691.

47 Qu Y, Vadivelu S, Choi L et al. Neurons derived from embryonic stem (ES) cells resemble normal neurons in their vulnerability to excitotoxic death. Exp Neurol 2003;184:326–336.

48 Tom VJ, Doller CM, Malouf AT et al. Astrocyte-associated fibronectin is critical for axonal regeneration in adult white matter. J Neurosci 2004;24:9282–9290.

49 Tan AM, Zhang W, Levine JM. NG2: A component of the glial scar that inhibits axon growth. J Anat 2005;207:717–725.

50 Pasterkamp RJ, Verhaagen J. Emerging roles for semaphorins in neural regeneration. Brain Res Brain Res Rev 2001;35:36–54.

51 Houlé JD, Reier PJ. Transplantation of fetal spinal cord tissue into the chronically injured adult rat spinal cord. J Comp Neurol 1988;269:535–547.

52 Yang Z, Suzuki R, Daniels SB et al. NG2 glial cells provide a favorable substrate for growing axons. J Neurosci 2006;26:3829–3839.

53 Busch SA, Hamilton JA, Horn KP et al. Multipotent adult progenitor cells prevent macrophage-mediated axonal dieback and promote regrowth after spinal cord injury. J Neurosci 2011;31:944–953.

54 Ketschek AR, Haas C, Gallo G et al. The roles of neuronal and glial precursors in overcoming chondroitin sulfate proteoglycan inhibition. Exp Neurol 2012;235:627–637.

55 Noble LJ, Donovan F, Igarashi T et al. Matrix metalloproteinases limit functional recovery after spinal cord injury by modulation of early vascular events. J Neurosci 2002;22: 7526–7535.

56 Goussev S, Hsu JY, Lin Y et al. Differential temporal expression of matrix metalloproteinases after spinal cord injury: Relationship to revascularization and wound healing. J Neurosurg 2003;99 (suppl):188–197.

57 Larsen PH, Wells JE, Stallcup WB et al. Matrix metalloproteinase-9 facilitates 7remyelination in part by processing the inhibitory NG2 proteoglycan. J Neurosci 2003;23:11127–11135.

58 Oh LY, Larsen PH, Krekoski CA et al. Matrix metalloproteinase-9/gelatinase B is required for process outgrowth by oligodendrocytes. J Neurosci 1999;19:8464–8475.

59 Uhm JH, Dooley NP, Oh LY et al. Oligodendrocytes utilize a matrix metalloproteinase, MMP-9, to extend processes along an astrocyte extracellular matrix. Glia 1998;22:53–63.

60 Pendleton JC, Shamblott MJ, Gary DS et al. Chondroitin sulfate proteoglycans inhibit oligodendrocyte myelination through PTPσ Exp Neurol 2013;247:113–121.

61 Filous AR, Tran A, Howell CJ et al. Entrapment via synaptic-like connections between NG2 proteoglycan+ cells and dystrophic axons in the lesion plays a role in regeneration failure after spinal cord injury. J Neurosci 2014;34: 16369–16384.

62 Sellers DL, Horner PJ. Instructive niches: Environmental instructions that confound NG2 proteoglycan expression and the fate-restriction of CNS progenitors. J Anat 2005; 207:727–734.

63 Horner PJ, Thallmair M, Gage FH. Defining the NG2-expressing cell of the adult CNS. J Neurocytol 2002;31:469–480.

64 McTigue DM, Wei P, Stokes BT. Proliferation of NG2-positive cells and altered oligodendrocyte numbers in the contused rat spinal cord. J Neurosci 2001;21:3392–3400.

65 McTigue DM, Tripathi R, Wei P. NG2 colocalizes with axons and is expressed by a mixed cell population in spinal cord lesions. J Neuropathol Exp Neurol 2006;65:406–420.

66 Zuo J, Ferguson TA, Hernandez YJ et al. Neuronal matrix metalloproteinase-2 degrades and inactivates a neurite-inhibiting chondroitin sulfate proteoglycan. J Neurosci 1998;18:5203–5211.

67 Duchossoy Y, Horvat JC, Stettler O. MMP-related gelatinase activity is strongly induced in scar tissue of injured adult spinal cord and forms pathways for ingrowing neurites. Mol Cell Neurosci 2001;17:945–956.

68 Lakka SS, Rajan M, Gondi C et al. Adenovirus-mediated expression of antisense MMP-9 in glioma cells inhibits tumor growth and invasion. Oncogene 2002;21:8011–8019.

See www.StemCellsTM.com for supporting information available online.

